On the mechanical response of hybrid Fiber Reinforced Concrete with recycled and industrial steel fibers

Antonio Caggiano
Universidad de Buenos Aires. Facultad de Ingeniería. INTECIN – CONICET.
Av. Las Heras 2214, C1127AAR, Buenos Aires, Argentina.
e-mail: acaggiano@fi.uba.ar

Paula Folino
Universidad de Buenos Aires. Facultad de Ingeniería. INTECIN (UBA-CONICET).
Av. Las Heras 2214, C1127AAR, Buenos Aires, Argentina.
email: pfolino@fi.uba.ar

Carmine Lima
Department of Civil Engineering, University of Salerno, via Giovanni Paolo II 132, 84084, Fisciano (SA), Italy.
e-mail: clima@unisa.it

Enzo Martinelli*
Department of Civil Engineering, University of Salerno, via Giovanni Paolo II 132, 84084, Fisciano (SA), Italy.
e-mail: e.martinelli@unisa.it

Marco Pepe
Department of Civil Engineering, University of Salerno, via Giovanni Paolo II 132, 84084, Fisciano (SA), Italy.
e-mail: mapepe@unisa.it

*Corresponding Author.

The final version of this manuscript is available in *Construction and Building Materials*.
https://doi.org/10.1016/j.conbuildmat.2017.04.160

ABSTRACT

This paper summarizes the results of an experimental program on "sustainable" cementitious composites internally reinforced with industrial and recycled steel fibers, the latter being recovered from waste tires and employed in substitution and/or addition of the industrial steel fibers. Specifically, six concrete mixtures including different amount of industrial/recycled steel fibers were produced and tested both in compression and bending. The obtained results confirm the promising prospects already observed by the authors in a previous study on concrete reinforced with recycled steel fibers obtained from waste tires. Furthermore, they clearly demonstrate that industrial fibers can be replaced by an equal amount of recycled ones without a significant decay in the relevant mechanical properties, provided that the recycled ones present adequate geometrical characteristics.

KEYWORDS: FRC, Waste Tires; Recycling, Sustainable Concrete, Hybrid Industrial-Recycled FRC; Post-cracking toughness.

1. INTRODUCTION

Plenty of researches aim at characterizing the mechanical behavior of cementitious composite with short fibers randomly dispersed throughout the matrix [1]. Relevant applications in this field are based on employing metallic [2], synthetic [3][4], glass [5], natural [6][7] and recycled [8] fibers. More recently, short reinforcing fibers modified with nanotechnologies have been also considered [9]. In principle, fibers can play a significant role in enhancing the post-cracking response and toughness of FRC. From both experimental and theoretical standpoints, several studies have been performed with the aim of investigating the mechanical properties of FRC [10][11]. Nevertheless, for many years the lack of international codes, standards and guidelines for designing FRCs limited their actual use in structural applications. As a matter of fact, in the past FRC was mainly employed for controlling non-structural aspects, such as cracking control, durability enhancements, etc. Incorporating fibers as reinforcement in partial substitution of classical steel rebars has increasingly been considered in the last two decades, as a result of the publication of many design guidelines and codes [12]. Among various codes and standards, the very recent fib new Model Code [13] represents one of the worldwide reference for the design of FRC.

Moreover, in recent years, a significant research effort focused on the suitability and efficiency of using various recycled materials and industrial by-products as sustainable concrete constituents [14][15][16]. In this regards, one of the most promising solution from both environmental and technical point of view is to reuse waste tires whom two main constituents can be potentially obtained from recycling. As a matter of fact, approximately 1.4 billion tons vehicle pneumatics are sold annually in the world and, consequently, many of them can be categorized as “end of life” tires [17]. Therefore, there are strong motivations for investigating solutions capable to reduce the negative environmental impacts of waste tires during their service life (from the acquisition of raw materials

through to the recycling processes of the exhausted tire) [18][19]. Specifically, several studies propose a Life Cycle Assessment (LCA) for quantifying the material and energy flows in the different life stages of tires [20][21]. LCA for unutilized scrap tires is commonly used to determine the most cost-effective waste conversion or reusing option [22][23]. From the technical point of view, the internal steel reinforcement of tires can be reused in partial to total replacement of industrial steel fibers commonly use in the so-called Fiber-Reinforced Concrete (FRC) [24][25], meanwhile, rubber particles can be employed as partial or total replacement of natural aggregates for obtaining a cementitious composite often referred to as "rubberized concrete" [26][27][28].

In the recent years, several researches focused on the possible employment of Recycled Steel Fibers (RSFs) derived from waste tires for structural concrete production [29][30][31][32][33][34][35][36][37][38][39][40]. As a matter of principle, these studies demonstrated that the geometrical characterization of the RSFs can be highly variable: they are generally characterized by a nominal diameter ranging between 0.1 and 2 mm with a corresponding average aspect ratio (i.e., length-to-diameter ratio) ranging between 20 and 150. These variations mainly depend on both the original source (i.e., tires typology) and recycling processes. However, based on the results available in the scientific literature [25][31], RSFs and Industrial Steel Fibers (ISFs) exhibited similar mechanical response, both in terms of tensile strength and matrix-to-fiber bond. Consequently, the resulting Recycled FRC post-cracking behavior can be highly influenced by the intrinsic geometrical characteristics of RSFs.

On the other hand, innovative studies on fiber-reinforced cementitious composites addressed the possible combination of different types of fibers (leading to the so-called Hybrid FRC, HyFRC) which can play a synergistic role in enhancing the post-cracking response of structural members [41].

In this context, the present study reports the results of an experimental research carried out at the STRuctural ENGineering Testing Hall (STR.ENG.T.H) of the University of Salerno (Italy), that

aims at investigating the post-cracking behavior of concrete reinforced with both industrial and recycled fibers obtained from waste tires (i.e., HyFRCs). First of all, a detailed geometrical characterization of the RSFs is executed. Then, several HyFRC mixtures were produced beyond three reference mixtures: plain concrete and FRCs with 100% of ISFs and RSFs, respectively. On these mixtures, the mechanical characterization of the pre and post cracking behavior of FRC was performed through four-point bending tests [42][43].

One of the main original aspects addressed in this paper is the investigation of the mechanical response of the aforementioned HyFRCs aimed at quantifying the effect of replacing industrial fibers with an equal amount (in weight) of recycled ones. As a matter of fact, in the authors' best knowledge only few experimental studies have been carried out so far on these kinds of FRCs since most of the studies mainly referred to the two "extreme" cases of FRC (i.e, 100% of ISFs or 100% of RSFs) considered in this paper.

2. MATERIALS AND METHODS

2.1. Materials

Recycled Steel Fibers from waste tires

The RSFs employed in the experimental campaign reported in this work were supplied by an Italian company that collects and recycles exhausted waste tires. Around 20 kg of RSFs were received at the laboratory: they present highly variable diameters and lengths and, moreover, they generally have irregular shapes (Figure 1).

First, fibers were cleaned and selected by separating some thicker pieces of steel, which were deemed not suitable for being used as spread reinforcement, and rubber particles (Figure 1). No further cleaning operations were performed as the supplied RSFs did not present oil or other substances that could affect bond with the cementitious matrix. Then, a detailed geometric characterization was performed on a sample of 2000 fibers. Specifically, the geometric characterization was performed by measuring (for each fiber) the following parameters:

- Fiber diameter (d_f): expressed in mm and measured by means of a micrometer (Figure 2); three diameters were measured (at the two ends and in the middle of the fiber) and an average value was determined for each RSF;
- Fiber length (l_f): expressed in mm and conventionally defined, in accordance with the CNR-204/2006 specifications [12], as the distance between the outer ends of a fiber;
- Developed length of the fiber (l_d): expressed in mm and conventionally defined, in accordance with the CNR-204/2006 specifications [12], as the total ("developed") length of the fiber along its axis;

- Curvature Index (*CI*): representing a shape index aimed at evaluating the curvatures (somehow a tortuosity index) of the fiber. It is expressed in percentage and can be calculated through the following expression:

$$CI = \frac{l_d - l_f}{l_d}. \quad (1)$$

If *CI* is equal to 0%, the RSF is completely stretched, otherwise *CI* equal to 100% indicates that the fiber if fully curved;

- Aspect ratio (λ): defined as the ratio between the fiber length (l_d) and its diameter (d_f).

Figure 3 reports the frequency distribution of the measured fiber diameter and highlights a multimodal (two/three) distribution: this can be attributed to the different origins of the waste tires from which the recycled fibers are derived (i.e., exhausted waste tires from different kinds of vehicles: cars, trucks, etc.). The resulting measurements highlight that the fiber diameter ranged between 0.11 and 0.44 mm. An average value of 0.25 mm and a median value of around 0.22 mm with a standard deviation of 0.07 mm were evaluated. As already observed in previous studies either performed by the Authors [25][34] or by other Research Groups [32], diameters are characterized by a multimodal distribution: this is probably due to the presence of tires from light and heavy vehicles disposed in the recycling plant.

Figure 4 summarizes the results obtained in terms of fiber length. As a matter of principle, the graph highlights that the observed frequency distribution (ranging from 6 mm to 74 mm) is characterized by an average value of 26.17 mm, a modal value of 20.00 mm (with a range of 18-21 mm) and a median value of 25.00 mm, with a standard deviation of 9.52 mm.

Unlike the fiber diameters, the fiber length presents a unimodal distribution, as already observed in previous studies carried out by the Authors [25][34]. The unimodal distribution of the results can be attributed to the shredding and cutting procedures performed within the recycling plant.

It is worth highlighting that the results obtained in term of fiber lengths are quite similar to the ones reported in similar studies (e.g., an average value in the range 26-30 mm is reported in [32]), whereas shorter fibers (with average length in the rage 15-18 mm) were employed in a previous study performed by the Authors [25].

Figure 5 reports a comparison between the frequency distribution of the fiber length (l_f) and developed fiber length (l_d): as expected, l_d are higher than the l_f. More in-depth considerations can be obtained by analyzing the results in terms of Curvature Index (*CI*). Figure 6 shows that *CI* is lower than 20% in almost 60% of the sampled fibers: this means that the RSFs used in the present study were quite aligned, with limited curls and/or twists. Moreover, the unimodal distribution can be justified by the recycling procedures adopted for the production of RSFs as in the case of the fiber lengths.

The geometric characterization of fibers was completed by analyzing the aspect ratio (λ). Figure 7 shows that λ is highly variable between 17.48 and 321.74, with average value of 109.5, modal value of 100, median value of around 101 and standard deviation of 45.55. The results obtained in term of aspect ratio are quite different with respect to those already obtained in the literature: average values around 45 were determined in a previous study performed by the Authors [25][34], whereas significantly longer fibers with average aspect ratio around 130 were considered in other works available in the literature [32].

Finally, Table 1 summarizes the aforementioned statistical data obtained for the geometrical characterization of the Recycled Steel Fibers.

Industrial Steel Fibers

Being produced on purpose to be employed as a spread reinforcement in FRC, Industrial Steel Fibers (ISFs) are characterized by standard dimensions with an optimized shape, featuring two end hooks.

The length of fibers typically employed in structural applications ranges between 6 and 70 mm, whereas diameters range from 0.15 mm to 1.20 mm [44].

ISFs type Wirand® FS7 [45] were used in this study: their geometric and mechanical properties are summarized in Table 2.

Fiber reinforced concrete mixtures

The concrete mixtures employed for all plain concrete and HyFRCs were produced by using Portland cement type CEM II/A-LL 42.5R in accordance with the EN 197-1 [46] and a water-to-cement ratio equal to 0.49. The fine aggregates (namely "sand") were characterized by a maximum nominal diameter equal to 2 mm meanwhile the coarse aggregates were divided in two fractions: Class 1 (*N1*) with a nominal diameter ranging from 2 to 10 mm and Class 2 (*N2*) with nominal diameter ranging from 10 to 20 mm. In addition, an acrylic-based superplasticizer was added to the mixtures in order to achieve the necessary workability (i.e., for obtaining a slump class consistency S3 [47]). Table 3 reports detailed information about the "reference" plain concrete matrix composition, which was kept unchanged in all the FRC mixtures described below:

- one FRC mixture made with 0.75 % in volume (i.e., about 60 kg/m^3) of Industrial Steel Fibers (ISFs);
- two mixtures prepared by replacing 50% (ISF = RSF = 30 kg/m^3) and 100% in weight of ISFs with Recycled Steel Fibers (RSFs);
- two further HyFRC mixtures prepared with an increasing amount of RSFs against a fix quantity of ISF. Specifically, HyFRC mixtures with 1.00 % and 1.25 % (in volume), respectively, were cast for investigating cases characterized by higher recycled fiber contents (i.e., 50 and 70 kg/m^3) added to a fixed amount of ISFs (30 kg/m^3).

The choice of fiber contents and the combinations of ISFs and RSFs outlined above were assumed keeping in mind the experimental results obtained in a previous experimental campaign [34], where the replacement of industrial fibers with an equal amount of recycled one led to a significant decay in the post-cracking response of FRC. Therefore, the present study was also intended at understanding if a higher amount of RSFs can somehow compensate the aforementioned decay. Table 4 reports the concrete mixtures composition in terms of fiber content: SFRC denotes the mixture with 100% of ISFs, RFRC indicates the one with 100% of RSFs, HyFRCs denotes the three mixtures produced with different combinations of ISFs and RSFs and the plain concrete mixture is labeled as REF. More specifically, the first column of Table 4 identifies the type of mixture (i.e., plain, SFRC, RFRC and HyFRC). Then, the second column reports the label of the mixtures defined as *iX-rY* providing the key information about the amount (expressed in kg/m^3) of industrial "*i*" and recycled "*r*" fibers. For instance, the label ''*i30-r30*'' refers to a mixture containing 30 kg/m^3 of ISFs and 30 kg/m^3 of RSFs. Then, "Fibers amount" columns indicate, both in terms of volume fraction and weight, the total amount of fibers (i.e., ISFs + RSFs). Finally, the last four columns in Table 4 report the weight of industrial and recycled fibers within the mixture and the relative percentage amount.

2.2. Methods

For each mixture, three cubes (150 mm x 150 mm x 150 mm) and three prismatic specimens (150 mm x 150 mm x 600 mm) were prepared. One cubic sample (labeled as "*plain*") was extracted from each mixture before adding fibers with the aim of observing the properties of the sole cement matrix and, hence, figuring out its contribution to the behavior of FRC.

In order to characterize the mechanical response of the produced FRCs, the cubic samples were tested in compression, while the prismatic ones were tested under four-point bending, as shown in Figure 8.

All tests were performed after 28 days of curing and, before performing the four-point bending tests, the prismatic specimens were notched in the middle for about 45 mm in depth. The geometry of the tested specimens is depicted in Figure 9.

Experimental tests were conducted according to the procedures described in UNI 11039-2 [43] and UNI EN 12390-3 [48], for bending and compression tests, respectively. Specifically, the four-point bending tests were performed in displacement control and dedicated transducers monitoring the Crack Tip Opening Displacement (CTOD) in the two sides of the notch tip were employed (Figure 10) in order to measure the average CTOD (i.e., $CTOD_m$).

3. RESULTS AND DISCUSSION

3.1. Compressive strength

Figure 11 summarizes the results of the compression tests performed on cubic samples on both plain and fiber-reinforced concrete mixtures. The results highlight that the unreinforced "*plain*" mixtures (light blue bars in Figure 11) are characterized by a certain variability (with a compressive strength ranging between 23 and 30 MPa), even though the mixture composition of the cement-based matrices was kept unchanged. The measured scatter can be explained by the intrinsic heterogeneity of concrete mixtures: as a matter of fact, it should be highlighted that the six mixtures herein analyzed were produced with six different batches. Moreover, as already documented in the scientific literature [49], the presence of fibers slightly influences the resulting compressive strength of FRCs. Specifically, increasing amounts of fibers (or higher aspect ratios) may enhance compressive strength of concrete up to a certain threshold, which mainly depends on the aggregates and cementitious matrix quality. However, a bigger amount of steel fibers (beyond that threshold) could have an adverse effect on the resulting compressive strength, thus generating a loss in strength.

In almost all the cases analyzed herein, the presence of the fibers leads to enhancing compressive strength between 5% and 10% (see the blue bars in Figure 11) with respect to the corresponding plain mixture. In fact, mixture *i30-r70* is the only exception to this general trend, as a slight reduction in strength (around 5%) was actually observed: this can be due to the high amount of fiber characterizing this mix (i.e., 1.25% in volume) in comparison with the other specimens (0.75% and 1.00%), thus confirming the effect of fibers on compressive strength already highlighted in the literature [49]. Moreover, the resulting concrete densities (Figure 12) shows a non-monotonic relationship with respect to the total amount of fibers: this further corroborates the observation that a

small amount of fibers may have a slightly positive effect of the matrix strength in compression, which disappears for higher fiber contents.

3.2. Four-point bending tests

Experimental observations

Figure 13 shows the experimental results derived from the four-point bending tests [42][43] aimed at characterizing the post-cracking flexural behavior of FRC mixtures under investigation. Specifically, Figure 13a to Figure 13f report the experimental curves in terms of vertical load (*P*) vs. average Crack Tip Opening Displacement (CTODm, representing the average of the two opposite CTOD measures). In each graph, the black line represents the mean curve (based on three tested samples), whereas the grey area indicates the range of variation of the resulting curves.

On the one hand, the *REF* (plain) concrete presents a brittle failure triggered by the formation of the first crack (Figure 13a). On the other hand, the *i60-r0* mix presents a post-cracking response (under bending loads) characterized by a significant improvement of toughness (Figure 13b): this is due to the well-known bridging action of the Industrial Steel Fibers [50][51][52].

The analysis of the curve reported in Figure 13f highlights the influence of the complete replacement of ISFs with an equal volume of RSFs: also in this case, referred to as *i0-r60*, the FRC is characterized by a similar post-cracking behavior with that corresponding to *i60-r0*. At first sight, this was a somehow "unexpected" result, as a significant decay in the post-cracking response was observed in a previous study [34] when ISFs were replaced with an equal amount of RSFs. A more in-depth analysis of both constituents' properties and resulting bending responses led to detecting the aspect ratio of fibers as the main responsible of the difference in results obtained in this study with respect to the ones reported in a previous study [34]. As a matter of fact, as already pointed out in section 2.1, the RSFs employed in the present research have an average aspect ratio significantly

(almost twice) higher than the ones adopted in [34]: therefore, the RFSs have a more efficient behavior. Moreover, it is worth highlighting that the results reported in this study and those obtained by the Authors in a previous study [34] cannot be directly compared. On the one hand, the matrices did not have the same composition, on the other hand, the total volume of fibers was significantly different: 0.75 % in this study (60 kg/m^3) and 0.50 % (40 kg/m^3) in [34]. Further investigations, both experimental and theoretical in nature, will be conducted with the aim to better clarify the influence of both the total amount and the aspect ratio of fibers in the resulting properties of hybrid FRCs. However, some deductions, based on experimental results available in the literature [31][32], are figure out at the end of the next subsection.

Similarly, also in the case of *HyFRCs* (i.e., *i30-r30, i30-r50, i30-r70*) the presence of RSFs in partial replacement of ISFs does not significantly affect the performance of FRC (Figure 13c to Figure 13e). Conversely, in mixtures *i30-r50* and *i30-r70* the performance has improved due to the higher total amount of fibers in comparison with the references SFRC (i.e., *i60-r0*) mix.

Design relevant properties

A more comprehensive and objective analysis can be conducted by considering the representative parameters defined by the UNI-11039 part 1 [42] and 2 [43]:

- First crack strength (f_{lf}):

$$f_{lf} = \frac{P_{lf} \cdot l}{h \cdot \left(b - a_0\right)^2} \tag{2}$$

where P_{lf} represents the first crack load (in N), b, h and l are the width (in mm), height (in mm) and span length (in mm) of the tested beam, respectively, while a_0 (in mm) represents the notch depth;

- Work capacity indices: U_1 and U_2 (energy absorption values) representing the areas under the vertical load *P-CTOD* curve in a representative range for the Serviceability Limit State (i.e., considering a CTOD ranging between $CTOD_0$ and $CTOD_0$ + 0.6 mm) and for the Ultimate State (i.e., considering CTOD ranges between $CTOD_0$ + 0.6 mm and $CTOD_0$ + 3.0 mm), respectively;
- Equivalent post-cracking strengths: the first ($f_{eq(0-0.6)}$) supposed to be significant for the Serviceability Limit State (evaluated as a function of the U_1 parameter) [43], whereas the second one ($f_{eq(0.6-3)}$) which is rather relevant for the Ultimate State (evaluated as a function of the U_2 parameter) [43];
- Ductility indices, D_0 and D_1, that can be determined with the following equations:

$$D_0 = \frac{f_{eq(0-0.6)}}{f_{lf}}. \quad (3)$$

$$D_1 = \frac{f_{eq(0.6-3)}}{f_{eq(0-0.6)}}. \quad (4)$$

Moreover, based on the ductility indices the post-cracking response of the FRC mixtures can be defined [42]:

- "softening", for D_0 and D_1 ranging between 0.5 and 0.9;
- "plastic", for D_0 and D_1 ranging between 0.9 and 1.1;
- "hardening", for D_0 and D_1 higher than 1.1.

Table 5 reports a summary of the aforementioned parameters determined for the FRC mixtures under investigation. In addition, Figure 14 and Figure 15 highlight the influence of the ISFs replacement with RSFs by reporting the variation of the first crack strength and ductility indices, respectively.

The results indicate that the presence of RSFs slightly increases the first crack strength (Table 5 and Figure 14). In fact, the reference SFRC (i.e., produced with 60 kg of ISFs) presents a first crack strength equal to 3.26 MPa meanwhile for both RFRC and HyFRC *i30-r30* produced with an equal amount of total fibers (i.e., 0.75%) higher values were registered. Moreover, also the HyFRC *i30-r50* and *i30-r70* mixtures, containing a higher total amount of fibers (i.e., 1% and 1.25%), present higher crack strength values in comparison with the reference *i60-r0* mixture. These results can be due to the higher steel area in the cross section developed by the RSFs for a fixed amount of volume: it is worth highlighting that the ISFs are characterized by a fiber length significantly higher than the RSFs (around 60%).

On the contrary, the results in terms of ductility indices (D_0 and D_1 in Table 5 and Figure 15) highlight that RSFs slightly reduce the FRC toughness. In fact the D_0 changes from 1.06 (for *i60-r0*) to 1.01 (for *i0-r60*) when the RSFs fully replace the ISFs and to 1.02 (for *i30-r30*) when ISFs are partially (50%) replaced. In order to recover this gap, a higher amount of RSFs was also considered as in the *i30-r50* and *i30-r70* mixtures, which were characterized by values of 1.06 and 1.08 of D_0, respectively (Table 5).

Based on these results, it can be concluded that the post-cracking behavior of SFRC, RFRC and HyFRC for small crack openings can be defined as a plastic type, as in all cases D_0 ranges between 0.9 and 1.1. Conversely, when it comes to the ductility index D_1, the presence of RSFs moves the post-cracking behavior from hardening (D_1 equal to 1.24 for *i60-r0*) to a plastic (with values ranging between 0.9 and 1.1 in all cases in which RSFs were used).

In the authors' understanding, the reduced (and almost negligible) decay in the post-cracking response observed when ISFs are (even totally) replaced by RSFs ought mainly to be attributed to the higher aspect ratio characterizing the latter (i.e., about 110). This argument is also supported by other experimental results available in the literature [31][32], in which two different RSFs were used and

tested under 4PB following the UNI 11039 specifications. Specifically, Aiello et al. [31] reported 4PB tests considering 100% replacements of ISFs with RSFs characterized by an aspect ratio (equal to 100), slightly lower than the one employed in the present study; similarly, Centonze et al. [32] reported results of similar tests carried out on FRC specimens with RSFs characterized by slightly higher aspect ratio (equal to 130).

In both cases the volume fraction of RSFs was 0.46 % and, hence, the amount of fibers was similar to the one employed by the authors a previous study of theirs [34]. Nevertheless, the decay in the post-cracking response observed both in [31] and [32] was much lower (e.g., D_0 and D_1 were 1.11 and 0.92, respectively, for 100% ISFs, whereas 0.99 and 0.69 were the corresponding values determined for 100% RSFs) than in their previous study [34]. This observation corroborates the authors' idea that the higher performance of RSFs obtained in this study is mainly related to their higher aspect ratio, rather than to the higher amount of fibers (0.75% in this study vs. 0.50% in [34]).

4. CONCLUSIONS

This paper presented the results of an experimental research aimed at investigating the mechanical behavior of concrete reinforced with both Recycled and Industrial Steel Fibers. Based on the results presented herein, the following observations can be highlighted:

- the geometric characteristics of RSFs depend on the original source (waste tires) and the procedure adopted for the recycling process: the type of exhausted tires (cars, trucks, and so on) defines the fiber diameter, meanwhile the processing procedures play a fundamental role on the definition of the fiber lengths (both the nominal and developed ones) and, consequently, affects the aspect ratio of recycled fibers;
- as expected, compressive strength is slightly influenced (5% to 10% with respect to the corresponding plain mixture) by the presence of fibers; specifically, as already documented in the literature, small amounts of fibers slightly increase the compressive strength, whereas this effect disappears for amount of fibers higher of a certain threshold;
- conversely, bending response is highly influenced by the fiber contribution in comparison with the plain mixture, as a significant increase in toughness and ductility was actually observed in the post-peak cracking behavior;
- FRCs with RSFs were characterized by a significant post-cracking toughness almost comparable with the one obtained for mixtures with only industrial ones;
- this initially “unexpected” result can be explained by considering that the RSFs employed in this study had an average aspect ratio (around 110), even higher than ISFs (around 60) and, hence, they were capable to replace ISFs in bridging the cracks opening within the concrete matrix;
- therefore, the results obtained in this study are more encouraging than the ones reported in a previous paper [34] by the authors: considerations also based on other researchers’

observations seem to justify the idea that the higher performance of RSFs highlighted in this study is mainly due to their higher aspect ratio (i.e., 110 vs. 47) with respect to the recycled fibers mentioned in [34];

- however, both partial and total replacement of ISFs with an equal amount of RSFs slightly reduce toughness and ductility indices, especially for small crack opening values (i.e., those related to the calculation of the ductility index D_0) in which the non-straight shape of RFSs have the main consequences;
- nevertheless, in all the cases the post-cracking response of FRC is not substantially affected by the presence of RSFs and, replacing ISFs with a higher amount of RSFs, reduces this gap;
- the presence of RSFs turns the post-cracking behavior of the FRCs from crack-hardening to crack-plastic one for high values of crack openings with a subsequent reduction in the D_1 index.

Finally, the results analyzed in this study further confirm the promising prospects emerging from previous studies on FRC with Recycled Steel Fibers derived from waste tires. The results clearly demonstrate that industrial steel fibers can be replaced by an equal (or slightly higher) amount of recycled ones without a significant decay in the relevant mechanical properties if the RSFs are characterized by adequate geometrical characteristics.

ACKNOWLEDGEMENTS

The authors are grateful to ‘‘*La.Sp.Ed. Tirreno Srl*’’ for their important support to the experimental investigation. ‘‘*RPN Tyres Srl*’’ is also acknowledged for having supplied the Recycled Steel Fibers used in the experimental campaign.

Finally, it should be highlighted that this study is part of the activities carried out by the authors within the “SUPERCONCRETE” Project (www.superconcrete-h2020.unisa.it), funded by the European Union within the Horizon 2020 Program (H2020-MSCA-RISE-2014 – n. 645704).

REFERENCES

[1] Di Prisco, M., Plizzari, G., Vandewalle, L. (2009). Fibre reinforced concrete: new design perspectives. Materials and Structures, 42(9), 1261-1281.

[2] Deluce, J.R., Vecchio, F.J. (2013). Cracking behavior of steel fiber-reinforced concrete members containing conventional reinforcement. ACI Structural Journal, 110(3), 481.

[3] Hesami, S., Hikouei, I. S., & Emadi, S. A. A. (2016). Mechanical behavior of self-compacting concrete pavements incorporating recycled tire rubber crumb and reinforced with polypropylene fiber. Journal of Cleaner Production, 133, 228-234.

[4] Soutsos, M.N., Le, T.T., Lampropoulos, A.P. (2012). Flexural performance of fibre reinforced concrete made with steel and synthetic fibres. Construction and building materials, 36, 704-710.

[5] Tassew, S.T., Lubell, A.S. (2014). Mechanical properties of glass fiber reinforced ceramic concrete. Construction and Building Materials, 51, 215-224.

[6] Ardanuy, M., Claramunt, J., Toledo Filho, R. D. (2015). Cellulosic fiber reinforced cement-based composites: a review of recent research. Construction and Building Materials, 79, 115-128.

[7] Ferreira, S. R., Martinelli, E., Pepe, M., de Andrade Silva, F., Toledo Filho, R. D. (2016). Inverse identification of the bond behavior for jute fibers in cementitious matrix. Composites Part B: Engineering, 95, 440-452.

[8] Foti, D. (2013). Use of recycled waste pet bottles fibers for the reinforcement of concrete. Composite Structures, 96, 396-404.

[9] Sobolev, K. (2016). Modern developments related to nanotechnology and nanoengineering of concrete. Frontiers of Structural and Civil Engineering, 10(2), 131-141.

[10] Gal, E., Kryvoruk, R. (2011). Meso-scale analysis of FRC using a two-step homogenization approach. Computers & Structures, 89(11), 921-929.

[11] Buratti, N., Mazzotti, C., Savoia, M. (2011). Post-cracking behaviour of steel and macro-synthetic fibre-reinforced concretes. Construction and Building Materials, 25(5), 2713-2722.

[12] CNR-DT 204/2006. Guide for the Design and Construction of Fiber-Reinforced Concrete Structures. ROME – CNR November 2007. Italian National Research Council.

[13] new *fib* Model-Code (2010) - First complete draft, Vol. 1 and 2. Comité Euro-International du Beton-Federation International de la Precontrainte, Paris.

[14] Paris, J. M., Roessler, J. G., Ferraro, C. C., DeFord, H. D., & Townsend, T. G. (2016). A review of waste products utilized as supplements to Portland cement in concrete. Journal of Cleaner Production, 121, 1-18.

[15] Pepe, M., Toledo Filho, R. D., Koenders, E. A., & Martinelli, E. (2016). A novel mix design methodology for Recycled Aggregate Concrete. Construction and Building Materials, 122, 362-372.

[16] Letelier, V., Tarela, E., Muñoz, P., & Moriconi, G. (2017). Combined effects of recycled hydrated cement and recycled aggregates on the mechanical properties of concrete. Construction and

Building Materials, 132, 365-375.

[17] European Tyre & Rubber Manufactures' Association (2010). End of life tyres - A valuable resource with growing potential, http://www.etrma.org/public/activitieseofltelts.asp .

[18] Wik, A., Dave, G. (2009). Occurrence and effects of tire wear particles in the environment–A critical review and an initial risk assessment. Environmental Pollution, 157(1), 1-11.

[19] Machin, E.B., Pedroso, D.T., de Carvalho, J.A. (2017). Energetic valorization of waste tires. Renewable and Sustainable Energy Reviews, 68, 306-315.

[20] Meyer, R., Benetto, E., Igos, E., Lavandier, C. (2016). Analysis of the different techniques to include noise damage in life cycle assessment. A case study for car tires. The International Journal of Life Cycle Assessment, 1-14.

[21] Rodríguez-Alloza, A.M., Malik, A., Lenzen, M., Gallego, J. (2015). Hybrid input–output life cycle assessment of warm mix asphalt mixtures. Journal of Cleaner Production, 90, 171-182.

[22] Fiksel, J., Bakshi, B.R., Baral, A., Guerra, E., De Quervain, B. (2011). Comparative life cycle assessment of beneficial applications for scrap tires. Clean technologies and environmental policy, 13(1), 19-35.

[23] Khoo, H. H. (2009). Life cycle impact assessment of various waste conversion technologies. Waste management, 29(6), 1892-1900.

[24] Aghaee, K., Yazdi, M.A., Tsavdaridis, K.D. (2014). Mechanical properties of structural lightweight concrete reinforced with waste steel wires. Magazine of Concrete Research, 66(1), 1-9.

[25] Caggiano, A., Xargay, H., Folino, P., Martinelli, E. (2015). Experimental and numerical characterization of the bond behavior of steel fibers recovered from waste tires embedded in cementitious matrices. Cement and Concrete Composites, 62, 146-155.

[26] Thomas, B.S., Kumar, S., Mehra, P., Gupta, R.C., Joseph, M., Csetenyi, L.J. (2016). Abrasion resistance of sustainable green concrete containing waste tire rubber particles. Construction and Building Materials, 124, 906-909.

[27] Thomas, B.S., Gupta, R.C., Panicker, V.J. (2016). Recycling of waste tire rubber as aggregate in concrete: Durability-related performance. Journal of Cleaner Production, 112, 504-513.

[28] Gupta, T., Chaudhary, S., & Sharma, R. K. (2016). Mechanical and durability properties of waste rubber fiber concrete with and without silica fume. Journal of Cleaner Production, 112, 702-711.

[29] Neocleous, K., Tlemat, H., & Pilakoutas, K. (2006). Design issues for concrete reinforced with steel fibers, including fibers recovered from used tires. Journal of materials in civil engineering, 18(5), 677-685.

[30] Papakonstantinou, C. G., & Tobolski, M. J. (2006). Use of waste tire steel beads in Portland cement concrete. Cement and Concrete Research, 36(9), 1686-1691.

[31] Aiello, M. A., Leuzzi, F., Centonze, G., & Maffezzoli, A. (2009). Use of steel fibres recovered from waste tyres as reinforcement in concrete: pull-out behaviour, compressive and flexural strength.

Waste Management, 29(6), 1960-1970.

[32] Centonze, G., Leone, M., & Aiello, M. A. (2012). Steel fibers from waste tires as reinforcement in concrete: a mechanical characterization. Construction and Building Materials, 36, 46-57.

[33] Graeff, A. G., Pilakoutas, K., Neocleous, K., & Peres, M. V. N. (2012). Fatigue resistance and cracking mechanism of concrete pavements reinforced with recycled steel fibres recovered from post-consumer tyres. Engineering Structures, 45, 385-395.

[34] Martinelli E., Caggiano A., Xargay H. (2015). An experimental study on the post-cracking behaviour of Hybrid Industrial/Recycled Steel Fiber-Reinforced Concrete. Construction and Building Materials, 94, 290-298.

[35] Zamanzadeh, Z., Lourenço, L., & Barros, J. (2015). Recycled steel fibre reinforced concrete failing in bending and in shear. Construction and Building Materials, 85, 195-207.

[36] Leone, M., Centonze, G., Colonna, D., Micelli, F., & Aiello, M. A. (2016). Experimental Study on Bond Behavior in Fiber-Reinforced Concrete with Low Content of Recycled Steel Fiber. Journal of Materials in Civil Engineering, 28(9), 04016068.

[37] Mastali, M., & Dalvand, A. (2016). Use of silica fume and recycled steel fibers in self-compacting concrete (SCC). Construction and Building Materials, 125, 196-209.

[38] Sengul, O. (2016). Mechanical behavior of concretes containing waste steel fibers recovered from scrap tires. Construction and Building Materials, 122, 649-658.

[39] Centonze, G., Leone, M., Micelli, F. & Aiello M.A. (2016). Mechanical properties of concrete reinforced with recycled steel fibers: a case study. In proceedings of the II international Conference on Concrete Sustainability ICCS16, Eds by J.C. Galvez, A. Aguado de Cea, D. Fernández-Ordóñez, K. Sakai, E. Reyes, M. J. Casati, A. Enfedaque, M.G. Alberti and A. de la Fuente, ISBN: 978-84-945077-8-6.

[40] Centonze, G., Leone, M., Micelli, F., Colonna, D.& Aiello M.A., (2016). Concrete reinforced with recycled steel fibers from end of life tires: mix design and applications", Proceedings of the 8th International Conference on Concrete Under Severe Conditions-Environment & Loading - Consec 2016, Lecco 12-14 sept. 2016, in Key Engineering Materials, Trans Tech Publication, ISSN:1013-9826, pp.224-231. doi:104028/www.scientific.net/KEM.711.224.

[41] Banthia, N., & Sappakittipakorn, M. (2007). Toughness enhancement in steel fiber reinforced concrete through fiber hybridization. Cement and Concrete Research, 37(9), 1366-1372.

[42] UNI-11039-1Steel Fiber Reinforced Concrete –Definitions, Classification and Designation, UNI Editions, Milan, Italy, 2003.

[43] UNI-11039-2Steel Fiber Reinforced Concrete – Test Method to Determine the First Crack Strength and Ductility Indexes, UNI Editions, Milan, Italy, 2003.

[44] ACI Committee 544 - ACI 544.1R-96. (Reapproved 2002). State-of-the-Art Report on Fiber Reinforced Concrete. Reported by ACI Committee 544.

[45] WIRAND® FIBRE FS7, Maccaferri TECHNICAL DATA SHEET Rev. 10, Date 08.11.2010.

[46] EN 197-1:2011 Cement Composition, specifications and conformity criteria for common cements.

[47] EN 12350-2:2009 Testing fresh concrete. Slump-test.

[48] EN 12390-4: 2009. Testing hardened concrete-Compressive strength of test specimens.

[49] Li, V. C. (1992). A simplified micromechanical model of compressive strength of fiber-reinforced cementitious composites. Cement and Concrete Composites, 14(2), 131-141.

[50] Mobasher, B., Stang, H., & Shah, S. P. (1990). Microcracking in fiber reinforced concrete. Cement and Concrete Research, 20(5), 665-676.

[51] Li, V. C. (2003). On engineered cementitious composites (ECC). Journal of advanced concrete technology, 1(3), 215-230.

[52] Barros, J. A., Cunha, V. M., Ribeiro, A. F., & Antunes, J. A. (2005). Post-cracking behaviour of steel fiber reinforced concrete. Materials and Structures, 38(1), 47-56.

Figure 1: Recycled steel fibers derived from waste tires.

Figure 2: Characterization of fibers: micrometer for the diameter measurements.

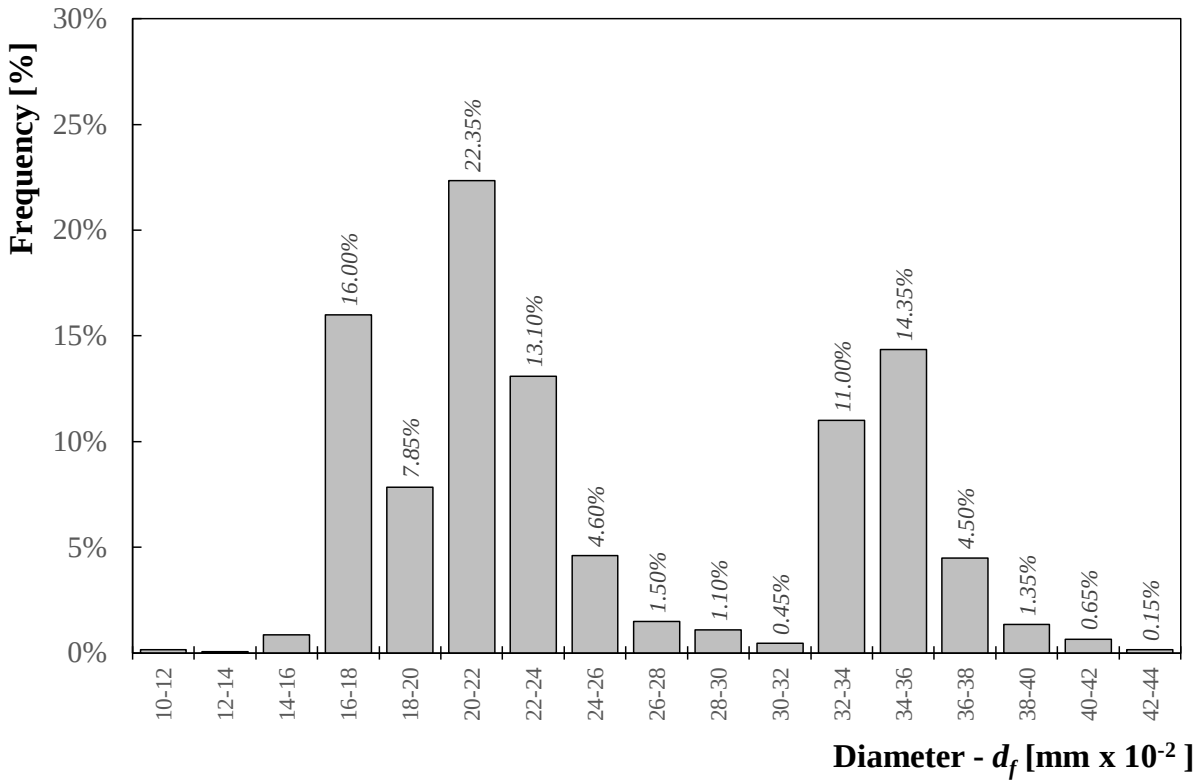

Figure 3: Frequency distribution of fiber diameter (d_f) measurements.

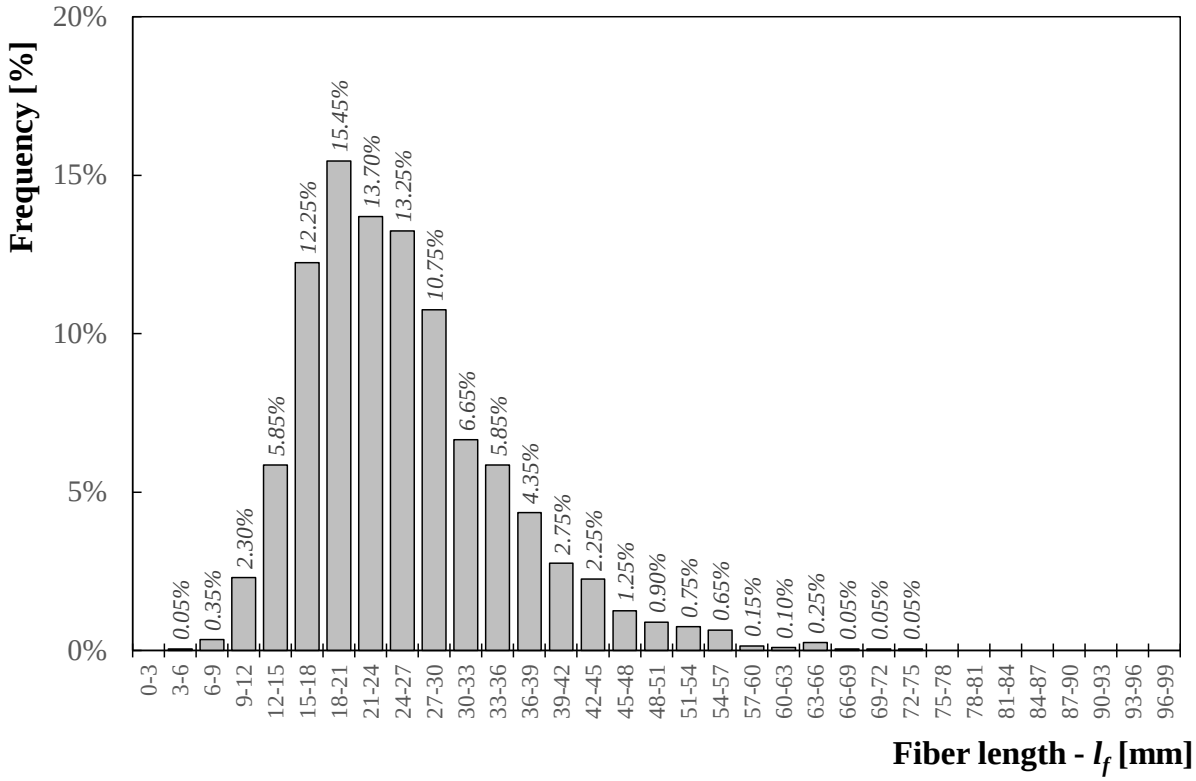

Figure 4: Frequency distribution of measured fiber lengths (l_f).

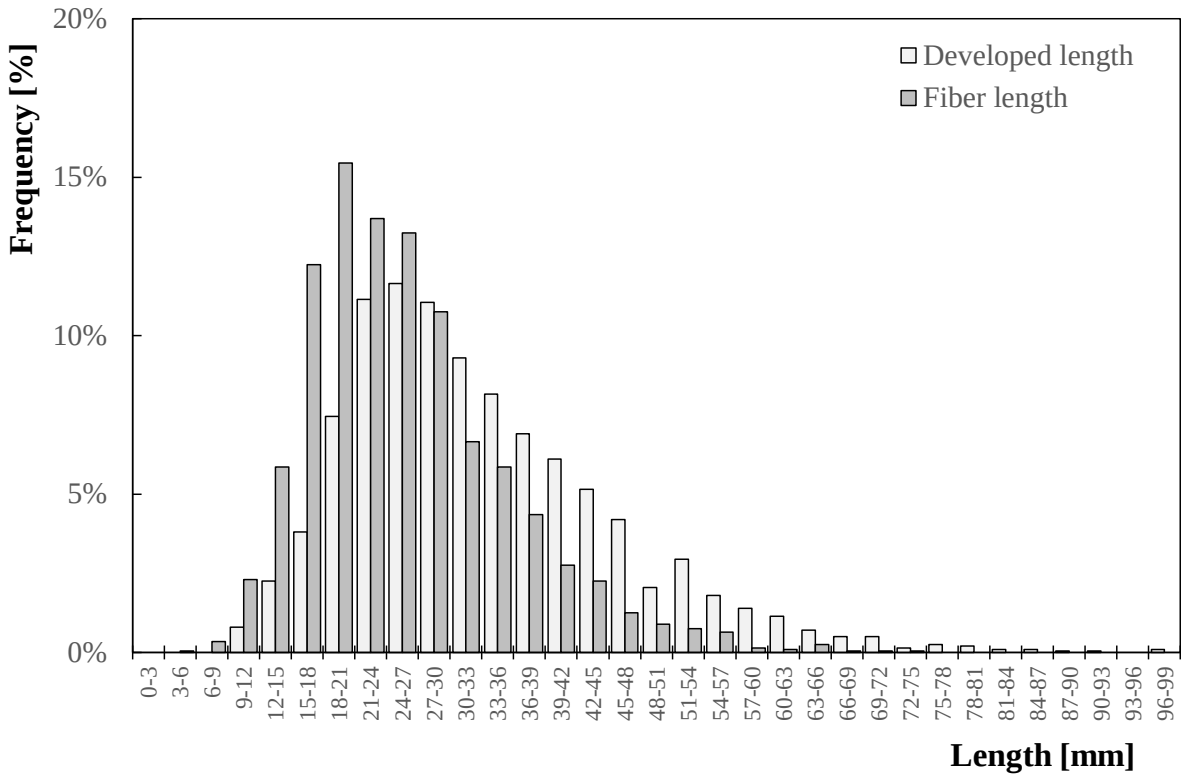

Figure 5: Frequency distribution of length (l_f) and development length (l_d) of the fibers.

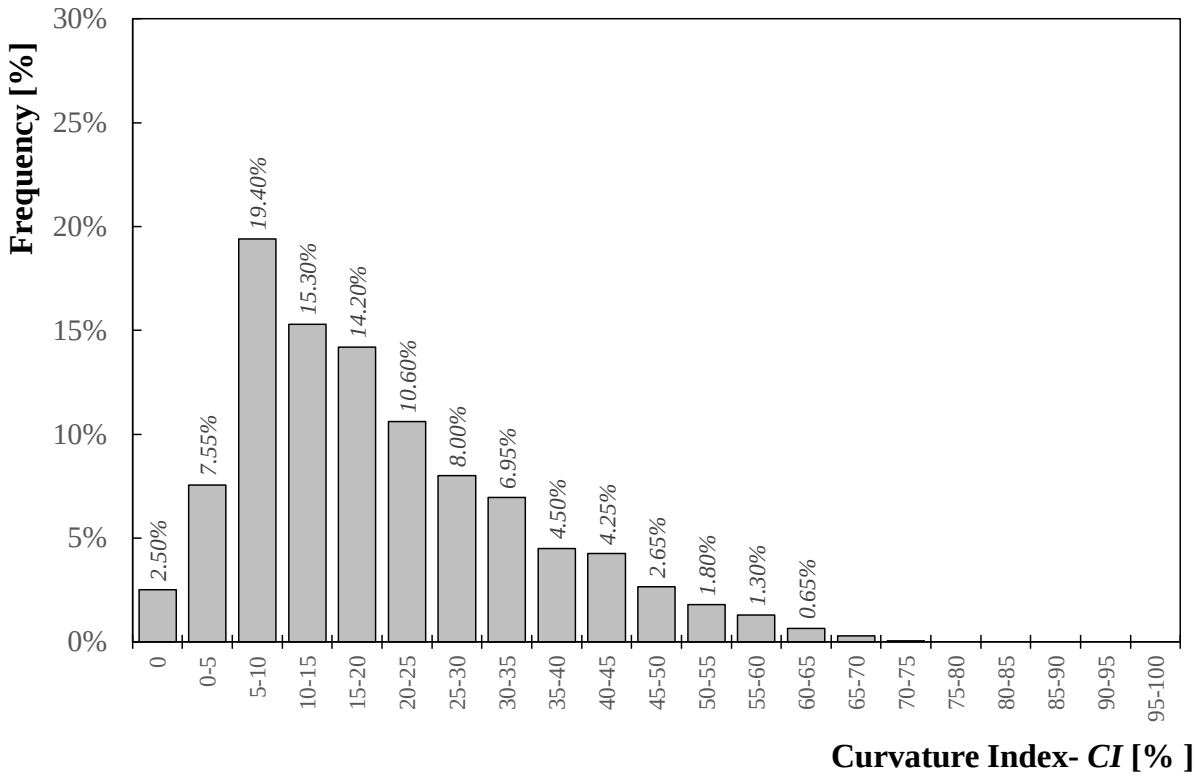

Figure 6: Frequency distribution of Curvature Index (CI).

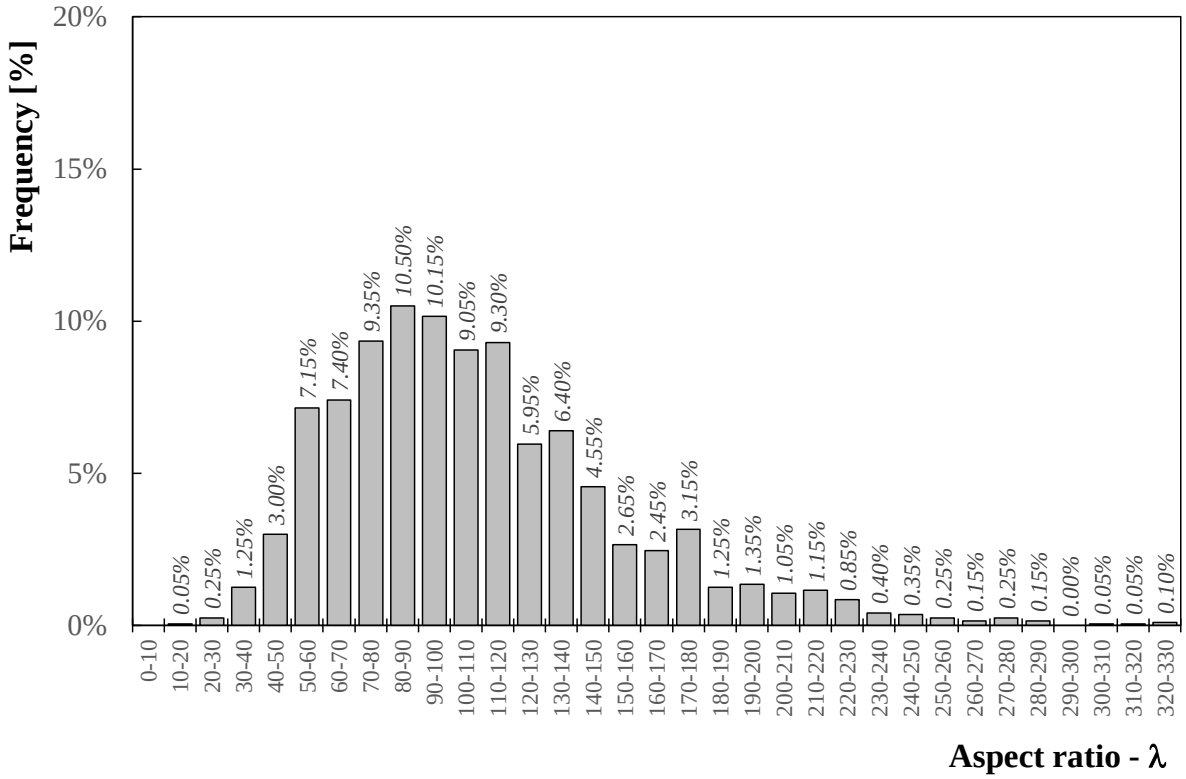

Figure 7: Frequency of the aspect ratio (λ).

Figure 8: Experimental set-up of the four-point bending test.

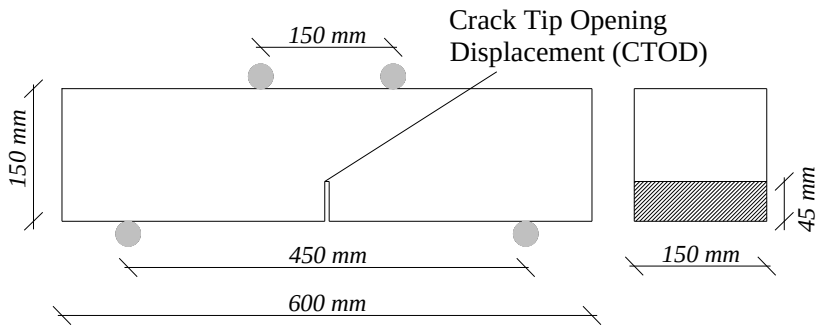

Figure 9: Geometry of the notched beam tested under four-point bending [43].

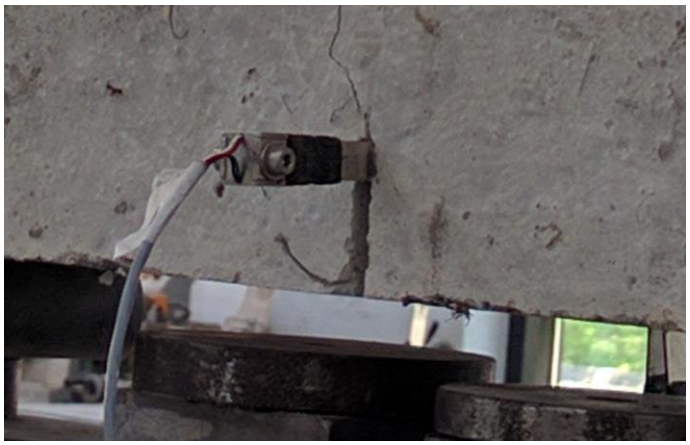

Figure 10: Detail of a transducer measuring the Crack Tip Opening Displacement (CTOD).

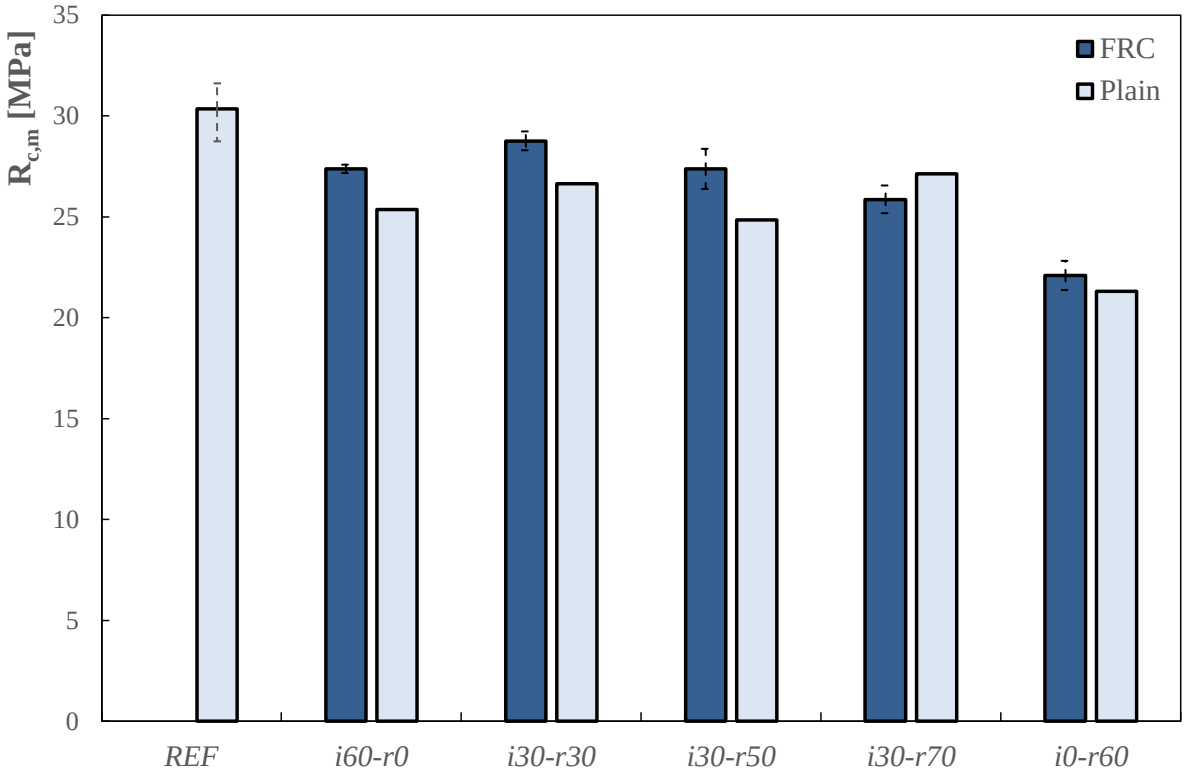

Figure 11: Cubic compressive strength measurements.

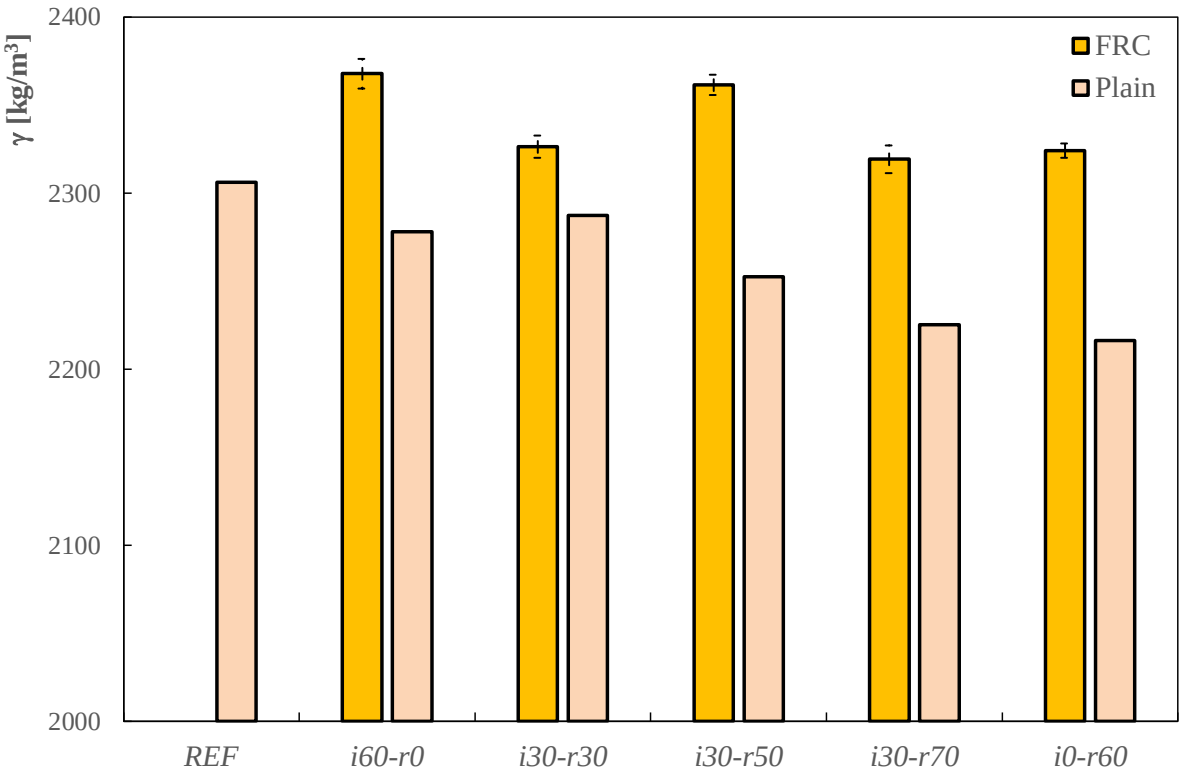

Figure 12: Density of hardened FRCs.

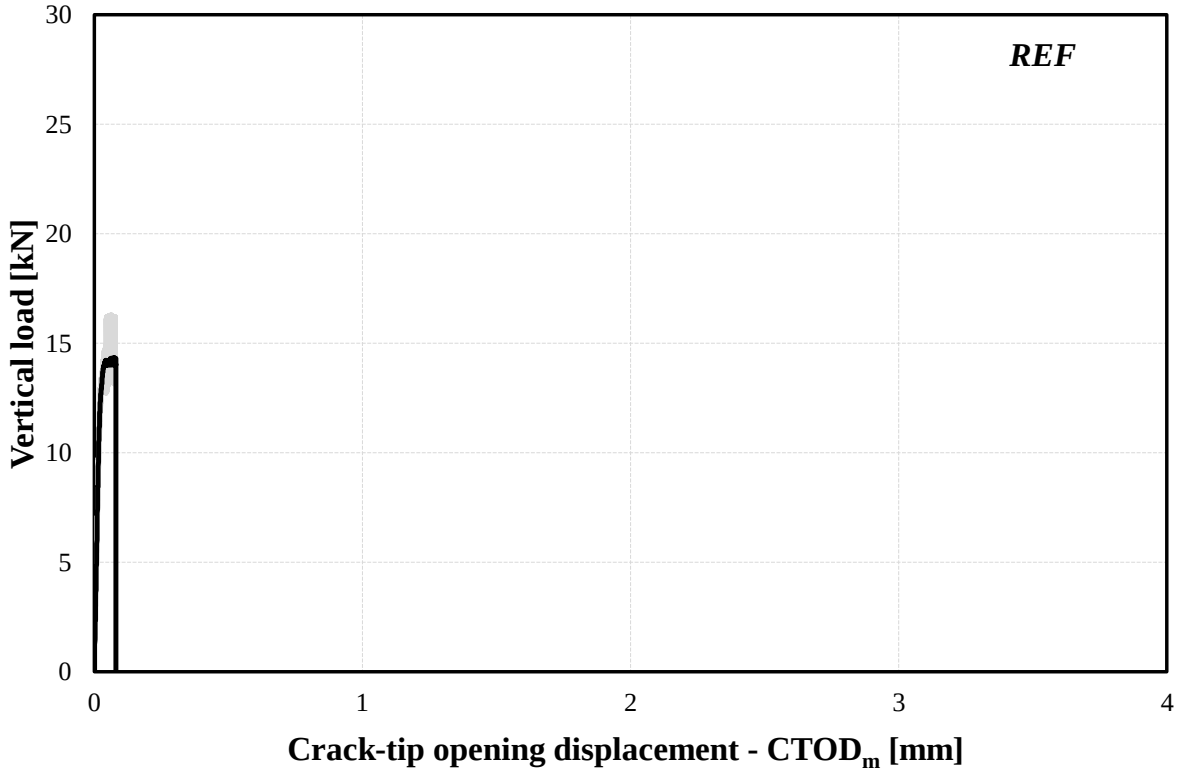

(a)

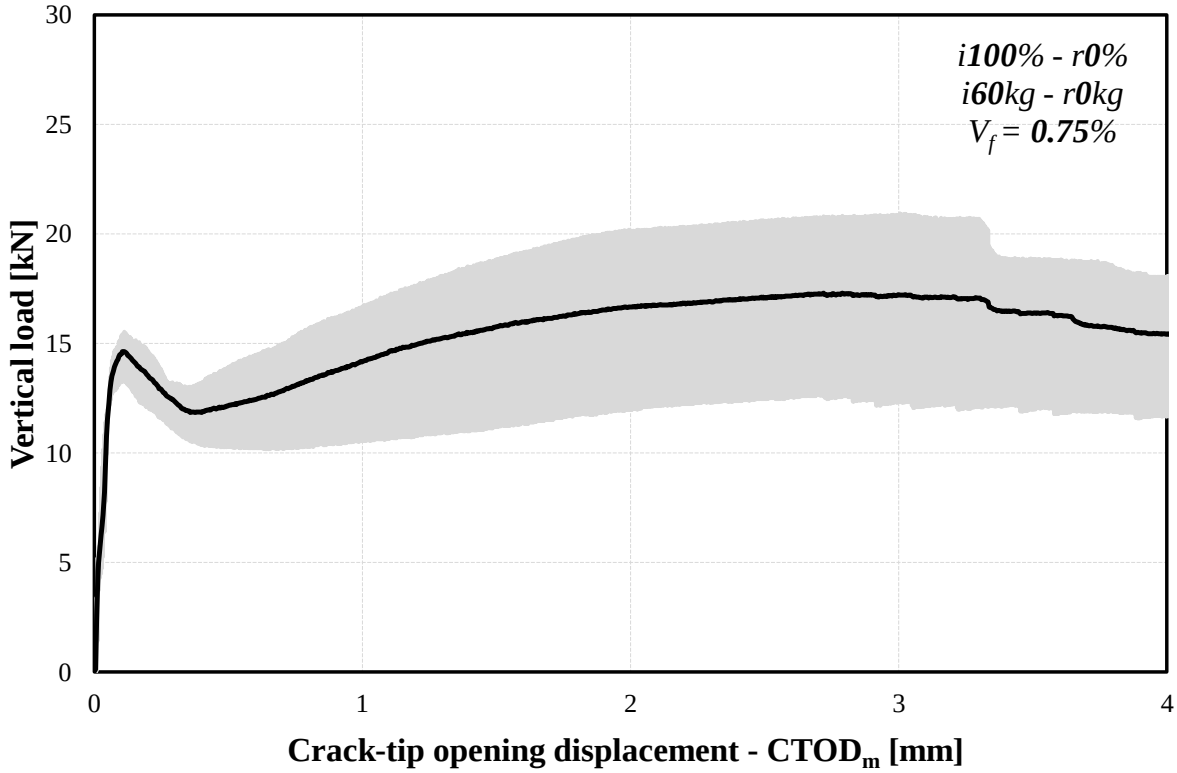

(b)

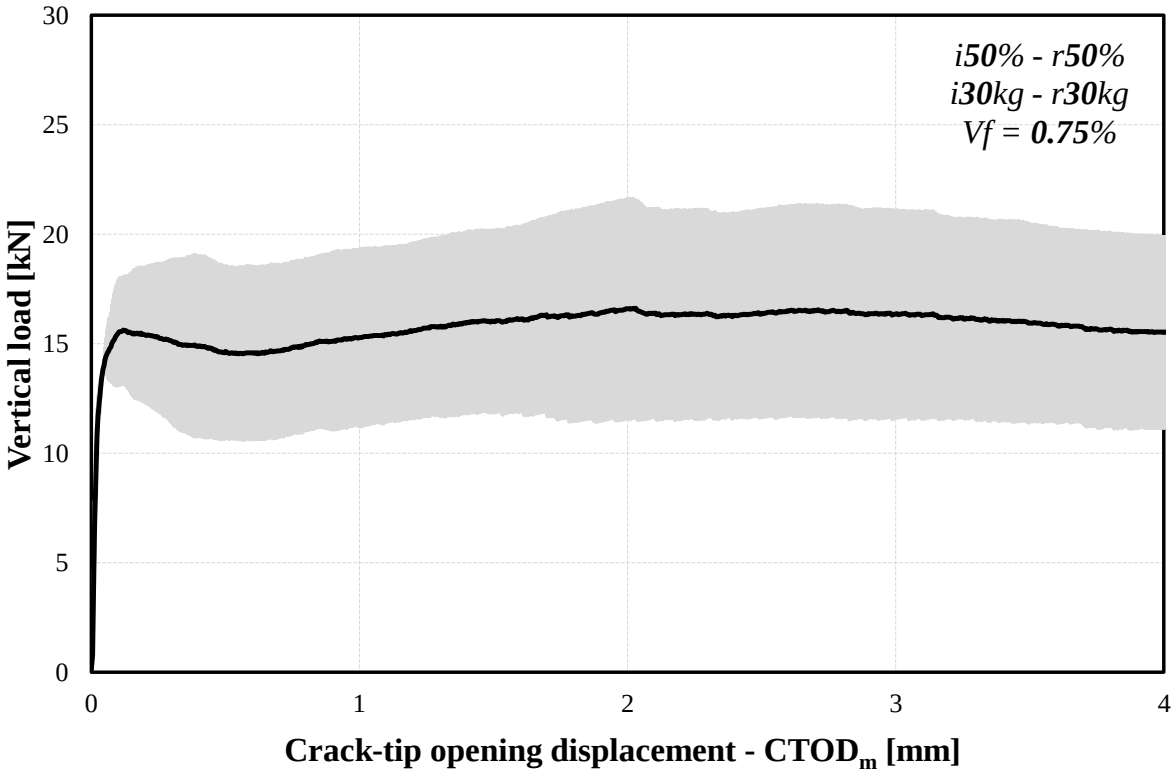

(c)

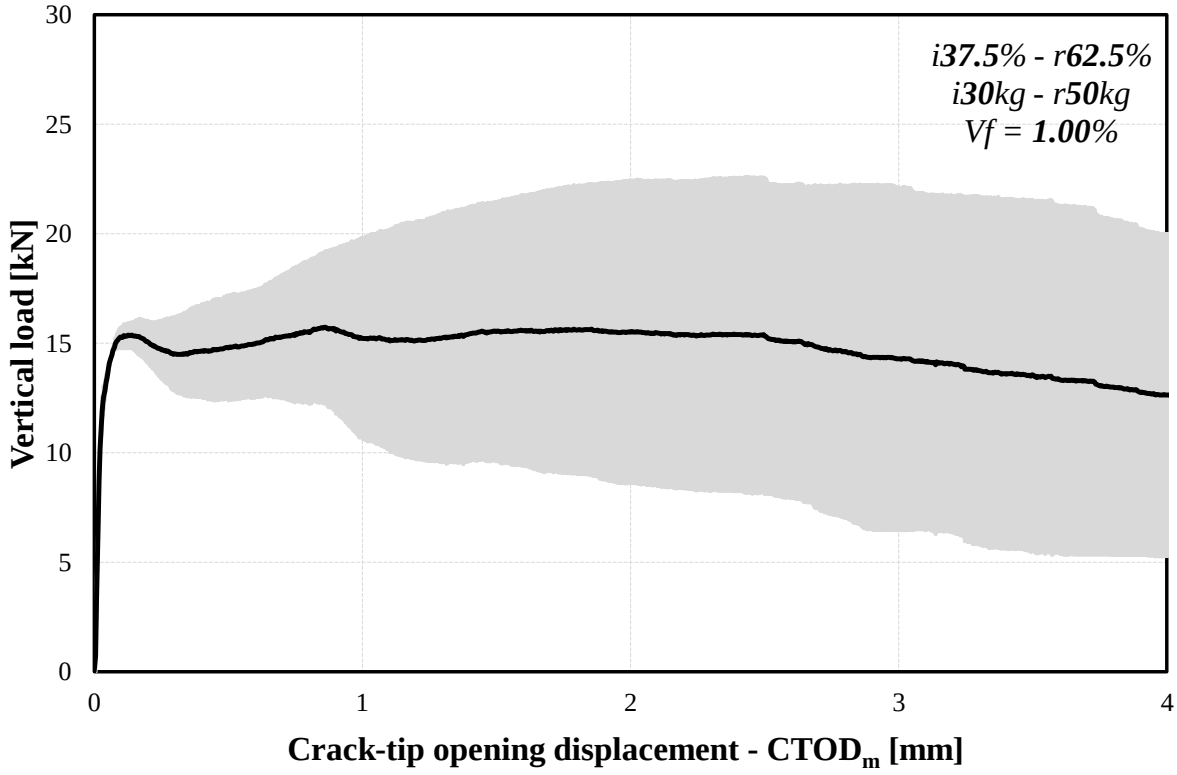

(d)

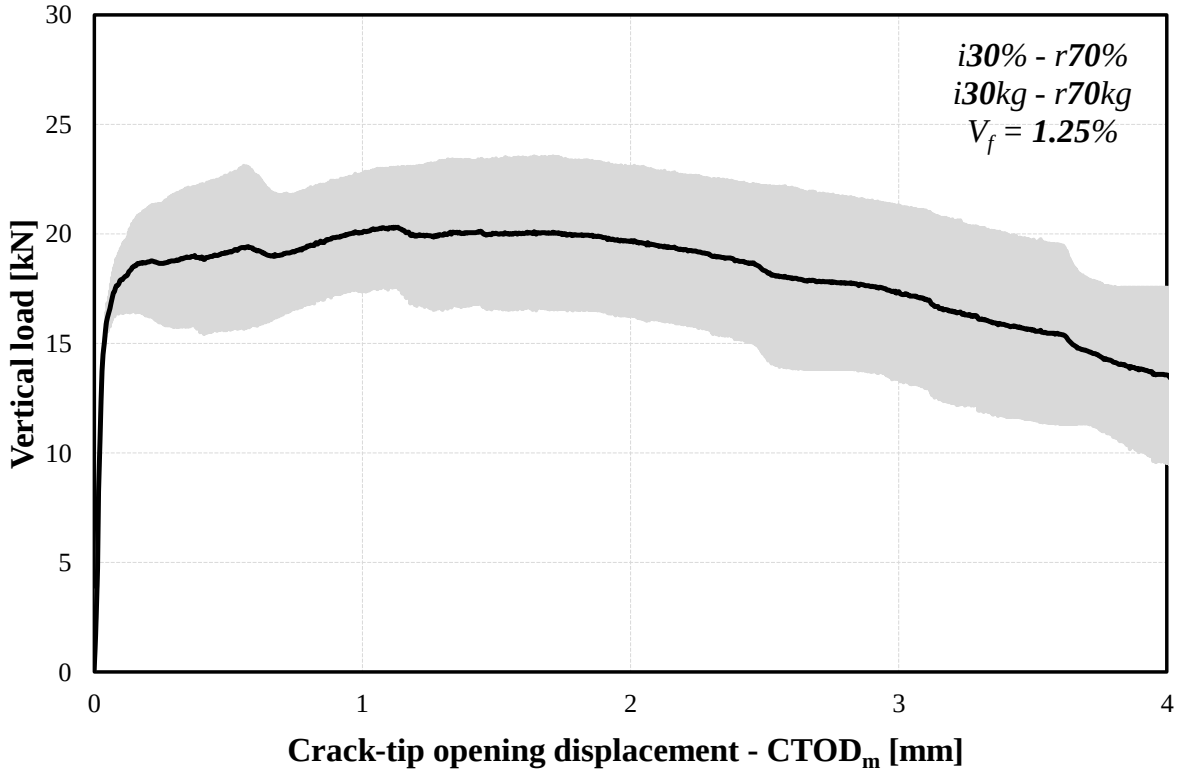

(e)

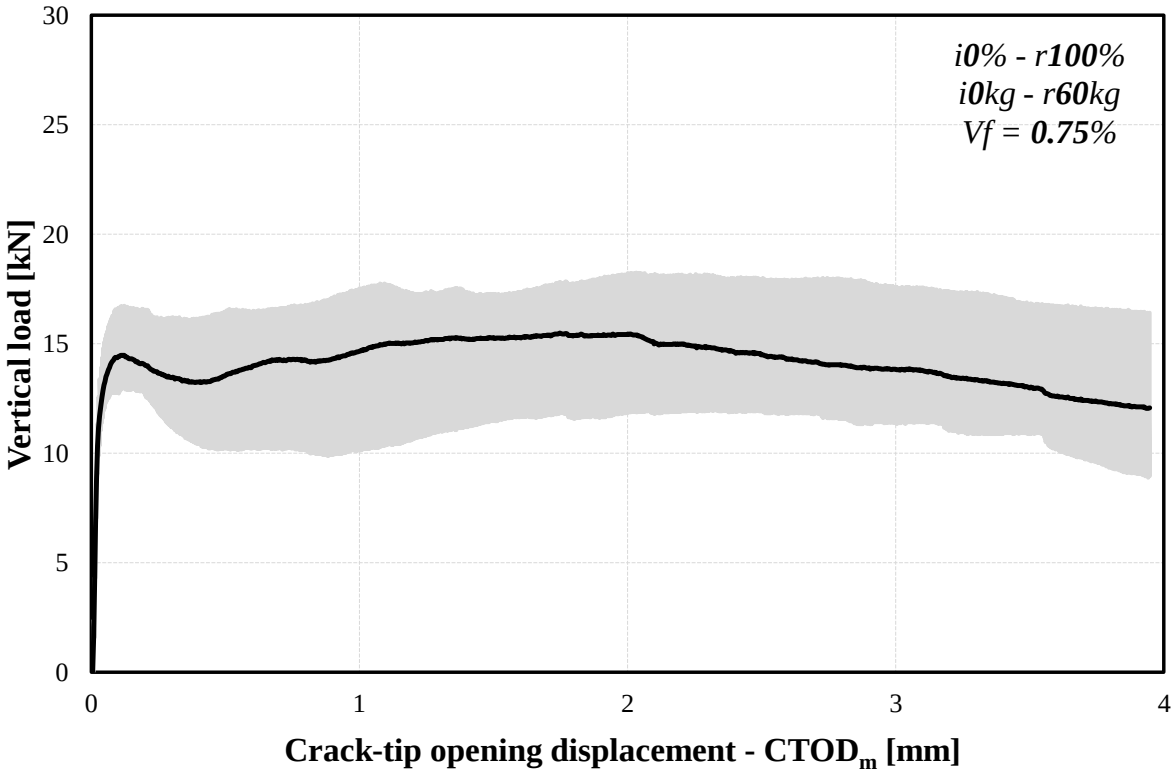

(f)

Figure 13: CTOD$_m$ – Vertical load.

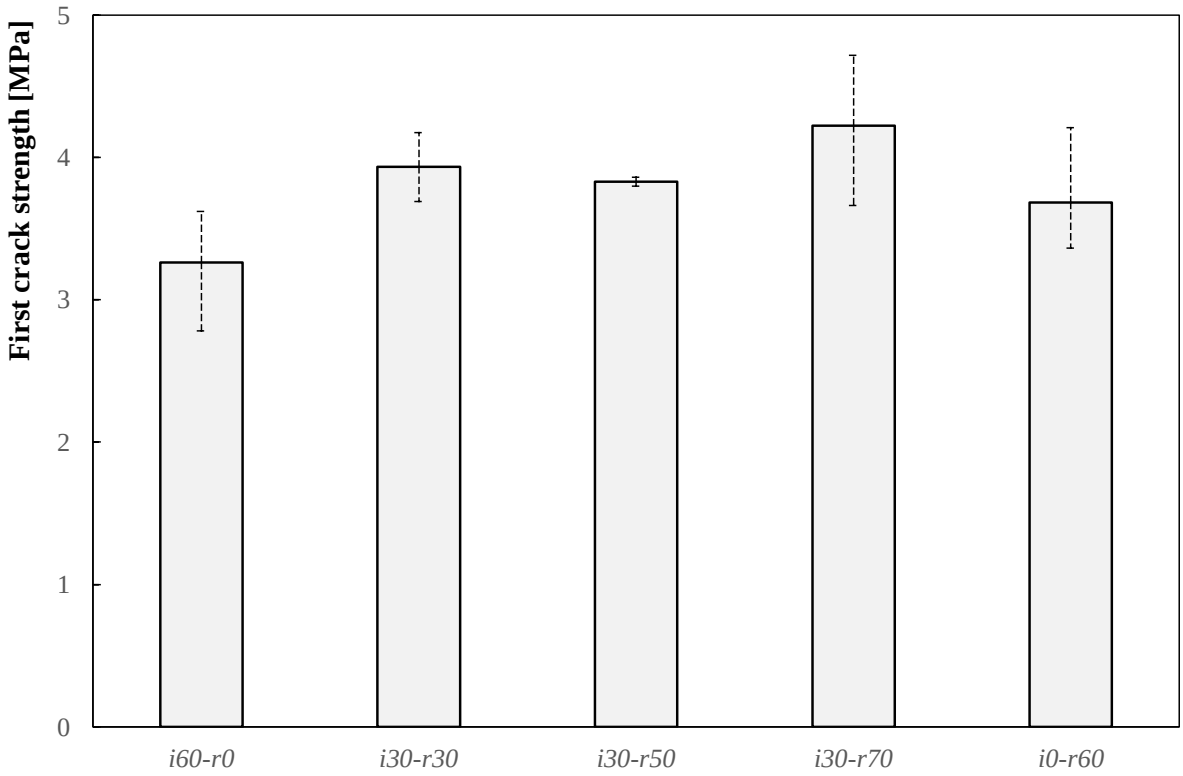

Figure 14: First crack strengths.

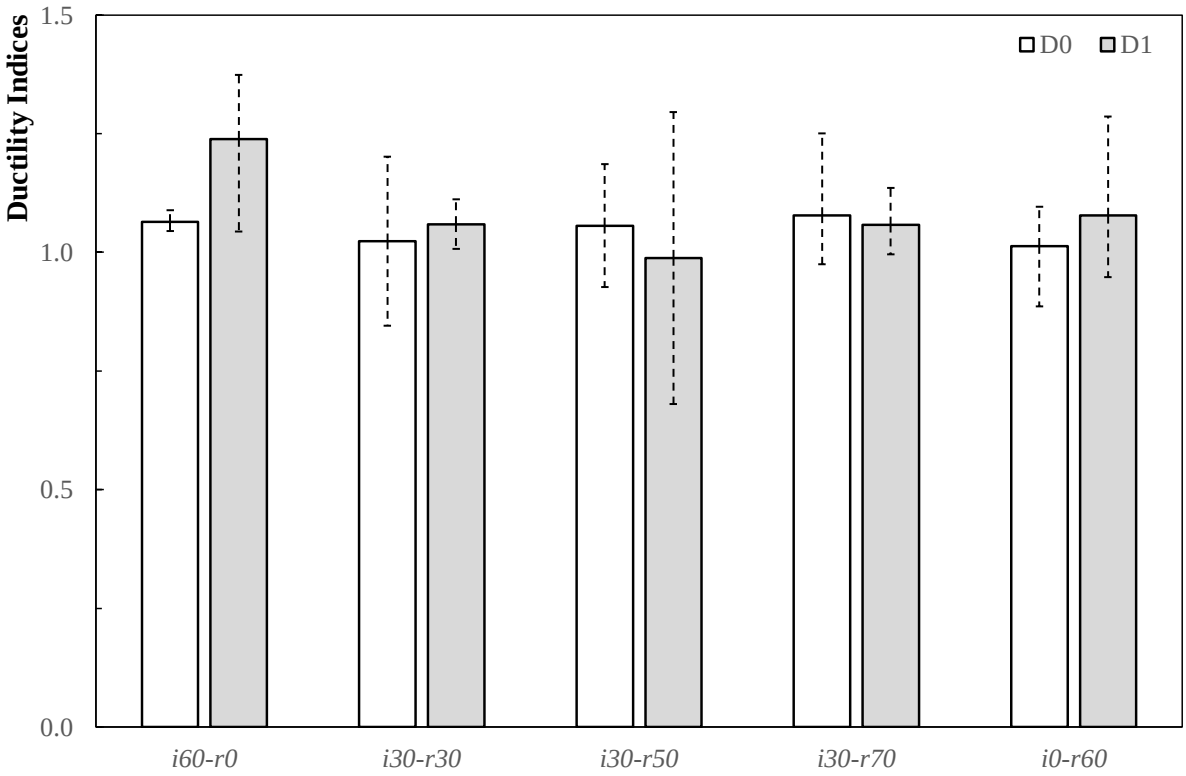

Figure 15: Ductility Indices according to UNI-11039-2 [43].

Table 1: Geometric characterization of RSFs from waste tires.

Parameter	Min	Max	Mode	Mode	Average	Median	Standard deviation
d_f [mm x 10^{-2}]	11.00	43.67	22.00	20-22	25.46	22.33	7.12
l_f [mm]	6.00	74.00	20.00	18-21	26.17	25.00	9.52
l_d [mm]	10.00	98.00	27.00	24-27	33.61	31.00	12.78
CI [%]	0.00	74.47	0.00	5-10	20.19	16.67	14.04
λ	17.48	321.74	100.00	90-100	109.05	101.74	45.55

Table 2: Geometric and mechanical properties of Wirand fibers FS7 [45].

Diameter [mm]	Length [mm]	Aspect Ratio	Tensile Strength [MPa]	Elastic Modulus [GPa]
0.55	33	60	> 1200	210

Table 3: Mixture composition (per cubic meter) of the cement-based matrix for plain concrete and FRCs.

Materials	Dosage [kg/m^3]
Sand	1012
Coarse aggregate N1	134
Coarse aggregate N2	764
Cement	320
Water	157
Superplasticizer (for plain mixture)	2.7
Superplasticizer (FRCs)	2.8-3.0

Table 4: FRC mixtures: fibers content and volume fraction.

Mixtures	Labels	Fibers amount [%]	Fibers amount [kg/m^3]	ISFs [kg/m^3]	RSFs [kg/m^3]	ISFs [%]	RSFs [%]
Plain	*REF*	0.00	-	-	-	0	0
SFRC	*i60-r0*	0.75	60	60	0	100	0
HyFRC	*i30-r30*	0.75	60	30	30	50	50
	i30-r50	1.00	80	30	50	37.5	62.5
	i30-r70	1.25	100	30	70	30	70
RFRC	*i0-r60*	0.75	60	0	60	0	100

Table 5: Post-cracking toughness and representative parameters (mean values).

Mixture	f_{lf} [MPa]	U_1 [kNmm]	U_2 [kNmm]	$f_{eq(0-0.6)}$ [MPa]	$f_{eq(0.6-3)}$ [MPa]	D_0 [MPa]	D_1 [MPa]
i60-r0	3.26	7.64	38.26	3.46	4.34	1.06	1.24
i30-r30	3.93	8.97	38.44	4.07	4.36	1.02	1.06
i30-r50	3.83	8.91	36.47	4.04	4.13	1.06	0.99
i30-r70	4.22	10.14	42.68	4.60	4.84	1.08	1.06
i0-r60	3.68	8.25	35.40	3.74	4.01	1.01	1.08